

# Adaptive Behavior of Double Concave Friction Pendulum Bearing and its Advantages over Friction Pendulum Systems

M. Malekzadeh<sup>1,\*</sup> and T. Taghikhany<sup>1</sup>

**Abstract.** *Double Concave Friction Pendulum (DCFP) bearing is a new generation of friction isolator that contains two separate concave sliding surfaces with different properties. Accommodating enhanced performance, compared to the Friction Pendulum System (FPS), is one of the most important benefits of DCFP. Herein, the seismic behavior of structures isolated by DCFP bearings is compared with the response of the same buildings using the FPS bearing. Accordingly, a series of nonlinear dynamic analyses are carried out under ensembles of ground motions at three different hazard levels (SLE, DBE and MCE). Moreover, the adaptive behavior of DCFP and its advantages in protecting secondary systems is investigated. The probability of exceedance curves of peak roof acceleration, peak inter-story drift and peak isolator displacement is compared for two types of isolation system. The result supports the advantages of DCFP isolation systems.*

**Keywords:** *DCFP; Friction pendulum systems; Base isolation.*

## INTRODUCTION

One of the most widely implemented and accepted seismic protection systems is base isolation [1,2]. The goal of base isolation is to simultaneously reduce inter-story drift and floor acceleration to limit or avoid damage not only to the structure, but also to its contents in a cost-effective manner.

Based on observations from the January 17, 1994 Northridge earthquake [3], some researchers have raised concerns as to the efficacy of seismic isolation during such events.

With reference to these reports, seismic isolated buildings located at near-fault sites are faced with very large displacements at the isolator level. To reduce these displacements, supplementary dampers are often prescribed. These dampers reduce displacements, but at the expense of significant increases in inter-storey drifts and floor accelerations in the superstructure [4].

The dilemma with regard to conventional isolation systems is the need to specify large amounts of

damping to mitigate very rare displacements, while this damping can be detrimental to the performance of the structure during occasional and rare events. A new innovative isolation system called Double Concave Friction Pendulum bearing, has the ability to progressively exhibit different hysteretic properties at different stages of displacement response [5,6].

This study is concerned with how this innovative isolation system can solve the dilemma related to conventional isolation systems, and enhance the seismic performance of isolated structures by exhibiting multi-stage behavior.

## SINGLE FRICTION PENDULUM BEARING

### Mechanism of Single Friction Pendulum Bearing

The single-concave friction pendulum bearing is the original Friction Pendulum System [7] and represents the first manufactured sliding bearing to make use of the pendulum concept. It is useful to recapitulate the essential aspects of their behavior, since the modeling of double FP bearings is an extension of the single-concave case.

The force-displacement relationship of single FP bearing has been modeled as a parallel arrangement

1. *Department of Civil Engineering, Amirkabir University of Technology, Tehran, Iran.*

\*. *Corresponding author. E-mail: malekzadeh.masoud@yahoo.com*

*Received 28 February 2009; received in revised form 26 September 2009; accepted 6 February 2010*

of a linear elastic spring element with stiffness based on the curvature of the spherical dish and a friction element with plasticity governed by a modified Bouc-Wen model [8,9].

The horizontal force,  $F$ , exerted by  $FP$  element is given by:

$$F = \frac{W}{R}u + \mu W Z, \quad (1)$$

where  $W$  is the weight carried by the bearing, and  $Z$  is a hysteretic variable ranging between  $[-1 \sim 1]$  that is governed by the differential Equation [9]:

$$\frac{dZ}{dt} = \frac{1}{u_y} \{A - |Z|^\eta [\gamma \text{sign}(\dot{u}Z) + \beta]\} \dot{u}, \quad (2)$$

where  $u_y$  is the yield displacement,  $u$  is the sliding velocity on the given surface and  $\gamma$ ,  $\beta$ ,  $\eta$  and  $A$  are dimensionless variables that control the shape of the hysteretic loop.

The coefficient of sliding friction is known to be velocity dependent [10], which can be modeled as:

$$\mu = f_{\max} - (f_{\max} - f_{\min}) \exp(-\alpha |\dot{u}|), \quad (3)$$

where  $f_{\max}$  and  $f_{\min}$  are the sliding coefficients of friction at large and nearly zero sliding velocities, respectively, and  $a$  is a rate parameter that controls the transition from  $f_{\min}$  to  $f_{\max}$ .

In addition to the elastic spring element and friction element, a gap component can be added in parallel to model the stiffening that occurs when contact is made with the displacement restrainer [11]. Zero force is exerted by the gap element for displacements below a predefined value. Beyond this displacement, the element behaves as a linear spring with large stiffness. This horizontal force which is made with a displacement restrainer is represented by:

$$F_r = K_r(|u| - d)\text{sign}(u)H(|u| - d), \quad (4)$$

where  $k_r$  is the stiffness exhibited by the displacement restrainer,  $d$  is the displacement capacity of the surface and  $H$  is the Heaviside step function.

## DOUBLE CONCAVE FRICTION PENDULUM BEARING

### Mechanism of Double Concave Friction Pendulum

Isolation bearings, such as the Friction Pendulum System (FPS), exhibit constant stiffness and damping under different hazard levels, and this behavior causes problems for design engineers to limit and control displacement at Maximum Credible Earthquake (MCE), while maintaining a good and desirable performance under more frequent and moderate seismic

events (SLE, DBE). To improve the performance of a FPS bearing subjected to small and moderate seismic events, an innovative friction bearing, termed Double Concave Friction Pendulum (DCFP), has been introduced [5]. This system is comprised of two sliding concave surfaces with an articulated slider. Figure 1 shows a typical Double Concave Friction Pendulum (DCFP). The DCFP bearing has several advantages over the FPS bearing, which are:

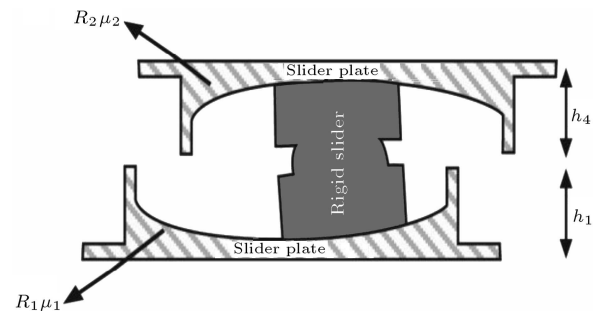
1. Lateral deformation is divided between the top and bottom concave surfaces and, consequently, the required plan diameter of each concave dish is significantly less than the equivalent Friction Pendulum System (FPS).
2. The Double Concave Friction Pendulum (DCFP) bearing exhibits desirable changes in stiffness and damping with an increasing amplitude of displacement.

The behavior and equations governing the force-displacement relationship of the double concave friction pendulum at each stage are summarized in Table 1. The dynamic characteristic of the DCFP bearing due to the action of two independent friction pendulum mechanisms is a function of the seismic input level.

The seismic behavior of the DCFP bearing is termed adaptive because its stiffness and damping vary in proportion to displacement amplitudes. This allows the design of the isolation system to be separately optimized for multiple performance objectives and multiple levels of input.

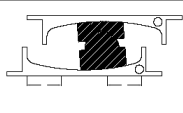
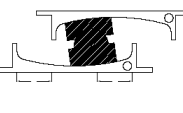
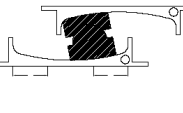
According to Figure 2, DCFP satisfies all the characteristics defined for a good isolation system. It means that the overall force-displacement relationship is very stiff at low input shaking, softens with increasing input, reaching minimum at the DBE and then stiffens again at higher levels of input [4].

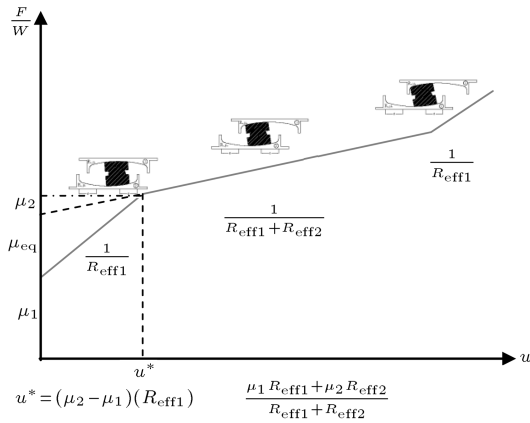
With reference to FPS bearings, there are just two target parameters that characterize the isolation performance at different hazard levels. However, in terms of the DCFP bearing, due to having two sliding surfaces that have different properties, a multi level



**Figure 1.** Section through a typical double concave friction pendulum.

**Table 1.** Summary of double concave friction pendulum bearing behaviour.

Figure	Stage	Force-Displacement Relationship
	Stage I: Sliding initiates on surface 1 but external force cannot overcome the friction on surface 2	$F = \frac{W}{R_{eff1}} u + F_{f1}$
	Stage II: External force overcomes the friction force along surface 2; sliding occurs on both surfaces	$F = \frac{W}{R_{eff1} + R_{eff2}} u + \frac{F_{f1}(R_{eff1}) + F_{f2}(R_{eff2})}{R_{eff1} + R_{eff2}}$
	Stage III: Slider contacts displacement restrainer on surface 2 and continues sliding on surface 1	$F = \frac{W}{R_{eff1}} u + F_{f1}$

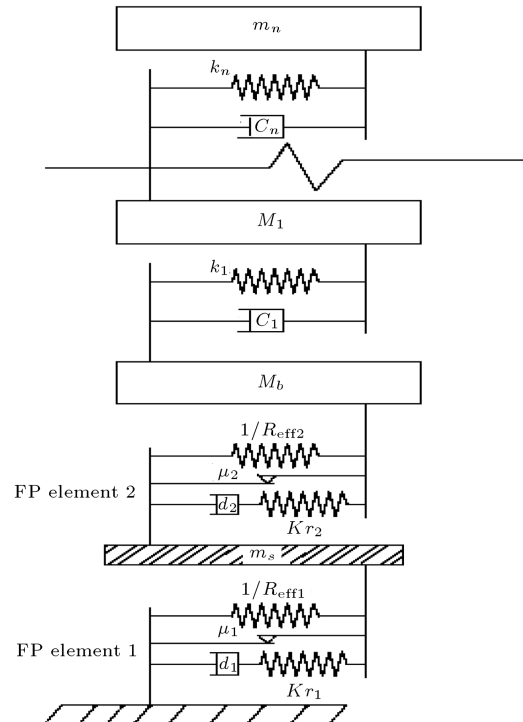

**Figure 2.** Overall force-displacement relationship of double concave friction pendulum.

performance of the system can be provided. In fact, design engineers are free to select different target parameters to undertake multi level designs and enhance the performance of the structure at different hazard levels, as recommended in performance based-design. As an advice approach, one can set lower concave parameters to characterize the isolation performance over low levels of excitation, while the performance of the isolation system over moderate and high levels of excitation can be defined by optimizing upper concave parameters.

### Mathematical Model

Recent studies show that the series model effectively simulates the hysteretic behavior of this novel isolation system [11]. In this mathematical model, the overall hysteretic behavior of DCFP is represented by two connected springs in series. In this section, a summary of previous work is presented to demonstrate how this mathematical model works [6,7]. The properties of

springs are related to the geometry of each concave respectively. Figure 3 shows a schematic of two single Friction Pendulum (FP) elements connected, in series, to model the overall hysteretic behavior of a double friction pendulum bearing. The small mass of the articulated slider is shown by  $m_s$ . Considering this small mass results in achieving displacements and velocities on each concave separately, which are the primary parameters in order to model each FP. Gap elements are included to simulate the stiffness exerted by the displacement restrainer beyond the displacement capacity. The mathematical description


**Figure 3.** Mathematical model of structure isolated with double concave friction pendulum.

of the bearing behavior has been previously published in report MCEER-00018 (Development, Implementation and Verification of Dynamic Analysis Models for Multi-spherical Sliding Bearings, August 2008). The report implemented the model in MATLAB and in SAP2000 and compared results to the shaking table test results. The mathematical formulation presented here (Equations 5 to 10) is the process used by Fenz in the report, in order to effectively model the hysteretic behavior of buildings isolated with a double concave friction pendulum. This process is represented here because an understanding of the mathematical modeling of a double concave friction pendulum bearing is fundamental for this study.

$F_i$  is the nonlinear force exerted by FP element  $i$  and represented by:

$$F_i = \frac{W}{R_{\text{eff}i}}(u_b - u_s) + \mu_i W Z_i + F_{r_i}, \quad (5)$$

where  $\mu_i$ ,  $Z_i$  and  $F_{r_i}$  are governed by the following equations:

$$\mu_i = f_{\max i} - (f_{\max i} - f_{\min i}) \exp(-\alpha |\dot{u}|), \quad (6)$$

$$Z_i Y_i = A_i (\dot{u}_b - \dot{u}_s) - |Z_i|^{\eta_2} (\gamma_i \text{sign}((\dot{u}_b - \dot{u}_s)) Z_i) + \beta_i (\dot{u}_b - \dot{u}_s), \quad (7)$$

$$F_{r_i} = K_{r_i} (|u_b - u_s| - d_i) \text{sign}(u_b - u_s) H(|u_b - u_s| - d_i). \quad (8)$$

For the articulated slider mass,  $m_s$ , the equation of motion is:

$$m_s (\ddot{u}_s + \ddot{u}_b) + F_1 - F_2 = 0. \quad (9)$$

Replacing  $F_{(i=1)}$  and  $F_{(i=2)}$  in Equation 9, an additional equation of motion can be obtained in the form of:

$$m_s (\ddot{u}_b + \ddot{u}_s) + \frac{W}{R_{\text{eff}1}}(u_s) + \mu_1 W Z_1 - \frac{W}{R_{\text{eff}2}}(u_b - u_s) - \mu_2 W Z_2 - F_{r_2} = 0. \quad (10)$$

For details of the theory and mathematical modeling of a double FP bearing, the reader is referred to previous papers in this field [5-7]. Here, by using the Runge-Kutta method and taking advantage of ODE functions (ode15s solver) that are introduced in the MATLAB Program [12], this differential equation is resolved numerically. In order to use the algorithm, three differential equations, which govern the state of motion related to the articulate slider, should be solved simultaneously at each step and, consequently, velocities, with the displacement of each surface, are computed individually.

## EARTHQUAKE GROUND MOTION

The study presented here set goals for investigating the multi-stage performance of structures using the DCFP bearing at different hazard levels. Achieving this goal requires ground motion time histories related to multiple hazard levels. As part of the SAC, the steel Project Somerville generates suites of time histories for use in performance based-design [13]. Suites of time histories are provided for three probabilities of occurrence: SLE (50% in 50 years), DBE (10% in 50 years) and MCE (2% in 50 years) and developed for Boston, Seattle and Los Angeles, which represent a range of seismic hazard levels from seismic zone 2 to zone 4. These records have a wide variety of intensities and frequency contents, providing an effective means of studying the multi-stage performance of a double FP bearing and comparing structures at different hazard levels. So, in this study, a suite of 60 time histories developed by Somerville et al for Los Angeles is used as input for nonlinear dynamic analysis. Table 2 presents the characteristics of records used in this study. These time histories are all derived from recordings of crustal earthquakes on soil category  $S_D$ . Eight of the DBE level time histories are near-fault recordings of strike-slip, oblique and thrust earthquakes in the magnitude range 6 to 7. The other two time histories for this level are the Landers and San Andreas earthquakes. The time histories used for the MCE level are derived from the 1974 Tabas, 1989 Loma Prieta, 1994 Northridge and 1995 Kobe earthquakes. Finally, the time histories for the SLE level are derived from earthquakes in the magnitude range 5.7 to 7.7 and the distance range of about 5 to 100 km.

Figure 4 shows 5% damped absolute acceleration response spectra for SLE, DBE and MCE levels.

## BEHAVIOUR OF DCFP BEARING UNDER DIFFERENT LEVEL EXCITATION

To show all possible sliding stages of a DCFP bearing, a single story building isolated with DCFP was investigated for three different level time-histories: LA56 (SLE-72 year), LA01 (DBE-475 year) and LA28 (MCE-2475 year). The DCFP properties are taken as:  $T_1 = 1.5$ ,  $T_{11} = 3.5$ ,  $\mu_{1 \min} = 0.02$ ,  $\mu_{2 \min} = 0.05$ ,  $\mu_{1 \max} = 0.04$ ,  $\mu_{2 \max} = 0.1$ ,  $d_1 = 127$  mm and  $d_2 =$  No limit (refer to Figure 1 and Table 3).  $d_1$  and  $d_2$  refer to the displacement capacity of the lower and upper concave, respectively.

Figure 5 shows the hysteretic behavior of the above DCFP bearing under selected multi level time histories.

As shown in Figures 5a, 5b and 5c, although the DCFP bearing is a fully passive device, its hysteretic behavior over different seismic hazard levels is compati-

**Table 2.** Characteristics of time histories.

SLE			DBE			MCE		
Record Label	Name	Amplitude Scale Factor	Record Label	Name	Amplitude Scale Factor	Record Label	Name	Amplitude Scale Factor
LA41	Coyote Lake	0.590	LA01	Imperial Valley	0.461	LA21	Artificial	1.283
LA42	Coyote Lake	0.333	LA02	Imperial Valley	0.676	LA22	Artificial	0.921
LA43	Imperial Valley	0.143	LA03	Imperial Valley	0.393	LA23	Artificial	0.418
LA44	Imperial Valley	0.112	LA04	Imperial Valley	0.488	LA24	Artificial	0.473
LA45	Kern County	0.144	LA05	Imperial Valley	0.302	LA25	Northridge	0.868
LA46	Kern County	0.159	LA06	Imperial Valley	0.234	LA26	Northridge	0.944
LA47	Landers	0.337	LA07	Landers	0.421	LA27	Northridge	0.927
LA48	Landers	0.308	LA08	Landers	0.426	LA28	Northridge	1.330
LA49	Morgan Hill	0.318	LA09	Landers	0.520	LA29	Tabas	0.809
LA50	Morgan Hill	0.546	LA10	Landers	0.360	LA30	Tabas	0.992
LA51	Parkfield	0.781	LA11	Loma Prieta	0.665	LA31	Artificial	1.297
LA52	Parkfield	0.632	LA12	Loma Prieta	0.970	LA32	Artificial	1.297
LA53	Parkfield	0.694	LA13	Northridge	0.678	LA33	Artificial	0.782
LA54	Parkfield	0.791	LA14	Northridge	0.657	LA34	Artificial	0.681
LA55	North Palm	0.518	LA15	Northridge	0.533	LA35	Artificial	0.992
LA56	North Palm	0.379	LA16	Northridge	0.580	LA36	Artificial	0.101
LA57	San Fernando	0.253	LA17	Northridge	0.569	LA37	Artificial	0.712
LA58	San Fernando	0.231	LA18	Northridge	0.817	LA38	Artificial	0.776
LA59	Whittier	0.769	LA19	North Palm	1.019	LA39	Artificial	0.500
LA60	Whittier	0.478	LA20	North Palm	0.987	LA40	Artificial	0.657

**Table 3.** Description of double concave friction pendulum design parameters.

Parameters	Description	Equation
$R_{eff1}$	Effective radius of curvature related to surface 1	$R_1 - h_1$
$R_{eff2}$	Effective radius of curvature related to surface 2	$R_2 - h_2$
$\mu_{eq}$	Effective coefficient of friction	$\mu_{eq} = \frac{R_{eff1}(\mu_1) + R_{eff2}(\mu_2)}{R_{eff1} + R_{eff2}}$
$T_I$	Period of system during first stage of sliding	$T_I = 2\pi \sqrt{\frac{R_{eff1}}{g}}$
$T_{II}$	Period of system during second stage of sliding	$T_{II} = 2\pi \sqrt{\frac{R_{eff1} + R_{eff2}}{g}}$

ble to the characteristic of input excitation and because of this fact, its behavior is called adaptive.

The bilinear behavior of the DCFP bearing is shown through Figure 5a under LA56. The behavior of this system under LA56, which relates to SLE with a return period equal to 74 years, is exactly the same as the single pendulum system. The external force generated by LA56 is just adequate enough to move the slider on a surface with a lower coefficient of friction. On the other hand, the external force is unable to overcome the friction force caused by the upper concave.

By increasing the seismic level up to DBE (LA01), the external force that excites the isolation system is

now capable of overcoming the friction force of both the upper and lower concave and due to this fact the hysteretic behavior of the DCFP changes to tri linear under LA01. The dash-line in Figure 4b makes the difference between Stage I and Stage II of sliding, which is described in Table 1.

Finally, along with an increasing level of excitation, Figure 5c represents the behavior of the DCFP bearing under LA28, which relates to the MCE seismic level with a return period of 2475 years. LA28 generates such a high external force that it moves the slider on both concaves up to the level where the slider contacts with the restrainer displacement on the lower concave causing an abrupt increase in stiffening.

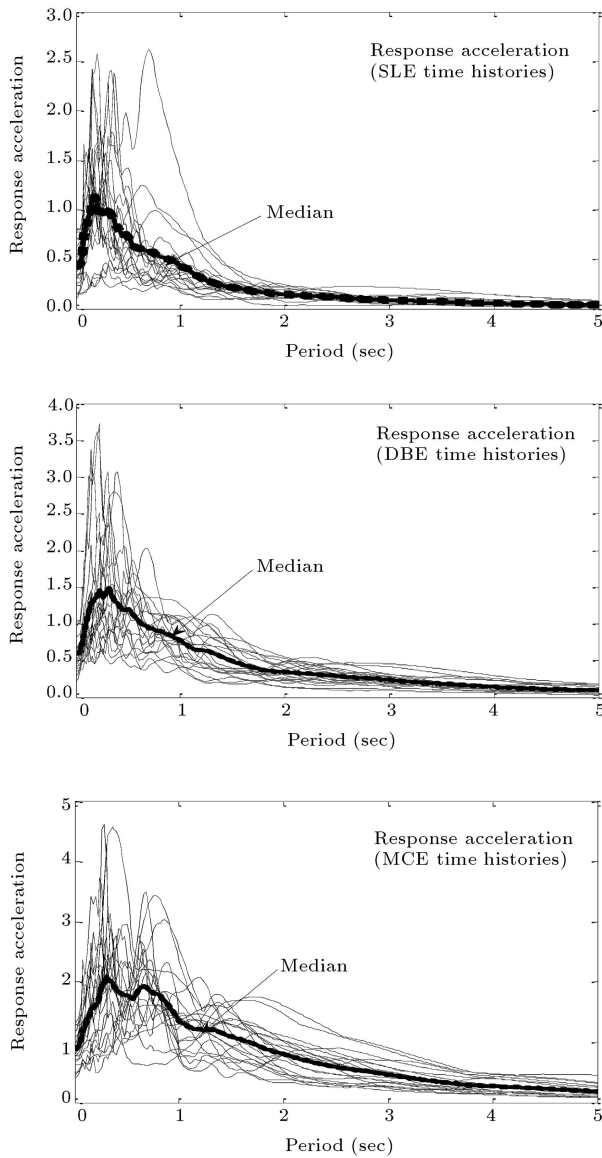


**Figure 4.** Acceleration response spectra of time histories ensembles.

Beyond this level, the slider continues sliding on the upper concave.

The dash-line in Figure 5c depicts an abrupt increase in the hysteretic behavior of the DCFP, due to contacting of the slider with the displacement restrainer of the lower concave.

In the following section, performances of FPS and DCFP bearings under different hazard levels are compared with each other.

**COMPARING SEISMIC PERFORMANCE OF FPS AND DCFP BEARINGS**

Herein, the seismic performance of isolated structures using FPS and DCFP bearings are compared under different seismic motion. The superstructure is assumed

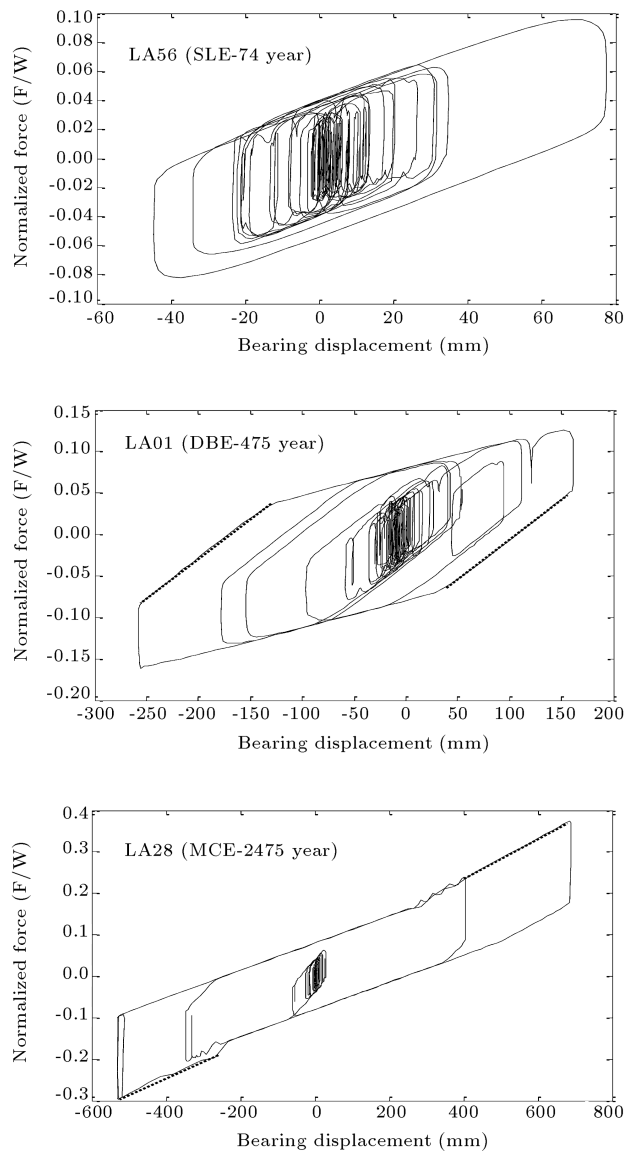


**Figure 5.** Multi stage performance of the double FP bearing under multi level time history.

as a one degree of freedom model with a natural period of 0.5 sec. The DCFP bearing is designed to exhibit the same median isolator displacements as the FPS bearing under the MCE hazard level (Table 4). Accordingly, the DCFP pendulum lengths were selected  $R_1 - h_1 = 101$  cm and  $R_2 - h_2 = 203$  cm, respectively. This corresponds to natural periods at each stage of sliding of  $T_1 = 2$  sec and  $T_2 = 3.5$  sec. Furthermore, for achieving the equivalent friction coefficient,  $\mu_{eq} = 0.093$ ,

**Table 4.** ASCE spectral parameters.

Name	$T_R$	$S_1$	$F_v$	$S_1 F_v$
SLE	72 year	0.0224 g	1.6	0.36 g
DBE	475 year	0.634 g	1.3	0.82 g
MCE	2475 year	1.13 g	1.3	1.47 g

friction coefficients for each top and bottom pendulum surface are selected as  $\mu_{1 \min} = 0.02$ ,  $\mu_{1 \max} = 0.04$  and  $\mu_{2 \min} = 0.06$ ,  $\mu_{2 \max} = 0.12$ .

In a single pendulum system (FPS), curvature radius is selected to exhibit a pendulum period of 3.5 sec (same as  $T_{II}$  for the DCFP system) and minimum and maximum friction coefficients are chosen as  $\mu_{\min} = 0.04$ ,  $\mu_{\max} = 0.08$  to generate the same equivalent friction coefficient of DCFP.

The nonlinear time-history analysis is conducted using a precise mathematical model for both systems under ensembles of ground motion (60 records in three categories: SLE, DBE and MCE).

The response quantities of interest are the roof absolute acceleration, the relative bearing displacement and the inter-story drift of the superstructure. Roof acceleration might be critical for rigidly attached equipment and braced ceiling systems. The relative bearing displacement is crucial from the design point of view of the isolation system. Structural inter-story drift is the response quantity of importance in the assessment of performance of nonstructural components such as vertical piping, cladding and architectural glass.

The median calculated values of peak absolute acceleration of the roof, the relative bearing displacement and the inter-story drift of the superstructure are summarized in Table 5 for each of the three hazard levels. The results indicate that these response parameters in the SLE level for a FPS isolated building between 25 to 33 percent are more than for the DCFP system, while the difference at the MCE level is negligible.

The probability of exceedance curves of peak roof acceleration, peak inter-story drift and peak isolator displacement are compared for two buildings isolated with FPS and DCFP in Figure 6. The results show that there is a significant reduction in the top floor acceleration of the building isolated with DCFP under SLE and DBE hazard levels, while the performance of both buildings during MCE is approximately the same.

In fact, double concave friction pendulum bearings not only protect structures against extreme earth-

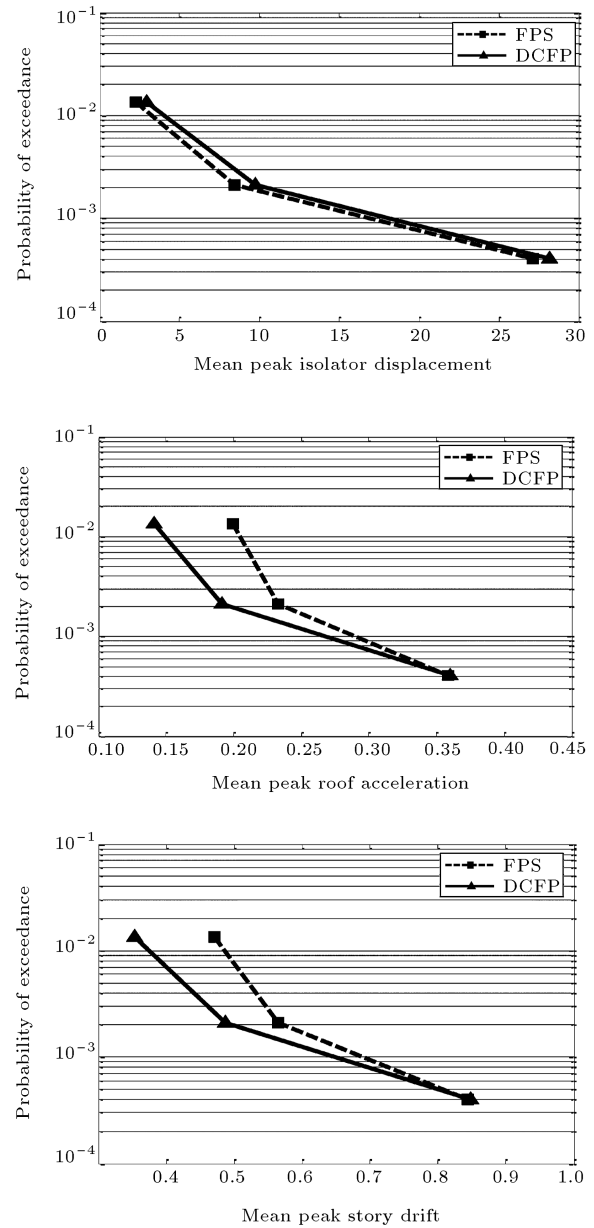


**Figure 6.** Median demand hazard curves for two buildings isolated with FPS and DCFP.

**Table 5.** Mean peak quantities of interest at three different hazard levels.

Hazard Level	Isolation Type	M.P.R.A*	M.P.S.D**	M.P.I.D***
SLE	FPS	0.1995	0.4712	2.23
	DCFP	0.1412	0.3532	2.94
DBE	FPS	0.2325	0.5653	8.449
	DCFP	0.1911	0.4872	9.76
MCE	FPS	0.3587	0.8441	27.11
	DCFP	0.3598	0.8486	28.2

\*M.P.R.A: Mean Peak Roof Acceleration; \*\*M.P.S.D: Mean Peak Story Drift;

\*\*\*M.P.I.D: Mean Peak Isolator Displacement.

quakes but also guarantee their performance during frequent and moderate seismic events at an acceptable level.

## CONCLUSION

The effectiveness of a recently developed isolation system, i.e. the double concave friction pendulum, for the vibration control of systems, has been investigated in this paper. Mathematical formulations involving differential equations have been proposed for analysis of the structure isolated by the DCFP subject to ground motions. This study has given an exposition of the dilemma in the design of the FPS system related to sacrificing performance during the more frequent, moderate seismic events in order to control and limit displacement under extreme earthquakes (MCE).

Two isolated structures with FPS and DCFP have been analyzed at three different hazard levels (SLE, DBE and MCE) under 60 records. The peak roof acceleration, peak inter-story drift and peak isolation displacement are considered as the response quantities of interest. Results exhibit approximately the same performance at the MCE level, however, at SLE and DBE levels, DCFP shows a significant reduction in the peak floor acceleration and peak inter-story drift of the super-structure in comparison to isolated buildings with the FPS bearing. In fact, DCFP acts as an adaptive isolation system, since stiffness and damping vary in proportion to the level of input ground motion, and can control peak floor acceleration and inter story drift together.

## REFERENCES

1. Naeim, F. and Kelly, J.M., *Design of Seismic Isolated Structures*, John Wiley & Sons Ltd., New York, NY. (1999)
2. Skinner, R.I., Robinson, W.H. and McVerry, G.H., *An Introduction to Seismic Isolation*, Wiley, Chichester, England (1993).
3. Hall, J.F. Ed. "Northridge earthquake of January 17, 1994 reconnaissance report", *Earthquake Spectra*, **11**, Supplement C, Vol. 1, pp. 173-198 (1995).
4. Kelly, J.M. "The role of damping in seismic isolation", *Earthquake Engineering and Structural Dynamics*, **28**(1), pp. 3-20 (1999).
5. Fenz, D.M. and Constantinou, M.C. "Behaviour of the double concave friction pendulum bearing", *Earthq. Engng. Struct. Dyn.*, **35**(11), pp. 1403-1422 (2006).
6. Fenz, D.M. and Constantinou, M.C. "Spherical sliding isolation bearings with adaptive behavior", *Theory, Earthquake Eng. Struct. Dyn.*, **37**, pp. 163-183 (2006).
7. Zayas, V.A., Low, S.S. and Mahin, S.A. "The FPS earthquake resisting system: Experimental report", Report No. UCB/EERC-87/01, Earthquake Engineering Research Center, University of California, Berkeley, CA, USA (1987).
8. Nagarajaiah, S., Reinhorn, A.M., Constantinou, M.C. "Nonlinear dynamic analysis of three-dimensional base isolated structures (3D-BASIS)", Technical Report NCEER-89-0019, National Center for Earthquake Engineering Research, Buffalo, NY, USA (1989).
9. Tsopelas, P.C., Roussis, P.C., Constantinou, M.C., Buchanan, R. and Reinhorn, A.M. "3DBASIS-MEM-B: Computer program for nonlinear dynamic analysis of seismically isolated structures", Technical Report MCEER-05-0009, Multidisciplinary Center for Earthquake Engineering Research, State University of New York at Buffalo, Buffalo, NY, USA (2005).
10. Constantinou, M.C., Mokha, A. and Reinhorn, A.M. "Teflon bearings in base isolation II: Modeling", *J. Struct. Eng., ASCE*, **116**(2), pp. 455-474 (1990).
11. Fenz, D.M. and Constantinou, M.C. "Modeling triple friction pendulum bearings for response-history analysis", *Earthquake Spectra*, **24**, pp. 1011-1028 (2008).
12. The MathWorks, Inc. MATLAB (Version 7.1), Natick, MA (2005).
13. Somerville, P., Anderson, D., Sun, J., Punyamurthula, S. and Smith, N. "Generation of ground motion time histories for performance-based seismic engineering", *Proc., 6th National Earthq. Eng. Conf.*, Seattle, Washington (1998).

## BIOGRAPHIES

**Masoud Malekzadeh** was born on 21st April, 1983 and, after graduation from the department of civil engineering at Tabriz University in 2006, continued his studies on earthquake engineering at Amirkabir University of Technology, Tehran, from where, in 2008, he received his MS degree. His research interests are earthquake engineering, performance based design, structural control and structural health monitoring.

**Touraj Taghikhany** was born on 13th November, 1969, in Tehran, Iran. After graduation from the department of civil engineering in Amirkabir University of Technology in 1993, he continued his studies on earthquake engineering at Sharif University of Technology, Tehran, and received his MS degree in 1996. He was awarded a PhD by the department of civil engineering and structural dynamics at Kyoto University (Japan) in 2004.

He then joined Amirkabir University of Technology in Tehran where he is, presently, an assistant professor of earthquake engineering. His current research is focused on the effect of near field ground motion on structures, earthquake engineering performance based probabilistic design, and application of control systems in structures.